IET Generation, Transmission & Distribution

Special Issue: Challenges and New Solutions for Enhancing Ancillary Services and Grid Resiliency in Low Inertia Power Systems

IET Journals
The Institution of Engineering and Technology

Advanced bidding strategy for participation of energy storage systems in joint energy and flexible ramping product market

ISSN 1751-8687
Received on 3rd February 2020
Revised 7th June 2020
Accepted on 11th June 2020
E-First on 9th July 2020
doi: 10.1049/iet-gtd.2020.0224
www.ietdl.org

Mohammad Khoshjahan[1] ✉, Moein Moeini-Aghtaie[2], Mahmud Fotuhi-Firuzabad[3], Payman Dehghanian[4], Hesam Mazaheri[3]

[1]*Department of Electrical and Computer Engineering, Texas A&M University, College Station, TX 77843, USA*
[2]*Department of Energy Engineering, Sharif University of Technology, Tehran, Iran*
[3]*Department of Electrical Engineering, Sharif University of Technology, Tehran, Iran*
[4]*Department of Electrical and Computer Engineering, George Washington University, Washington, DC 20052, USA*
✉ *E-mail: mohammad.khoshjahan@ieee.org*

Abstract: Recently, power system operators have initiated procurement of a new service in electricity markets named flexible ramping product (FRP). With the main goal of enhancing the grid flexibility, this product can provide a remarkable opportunity for an enhanced short-term profitability. Energy storage systems (ESSs) with high ramping capability can leverage their profitability when properly participating in this market. This study introduces a stochastic optimisation framework for participation of ESSs in the FRP market. The proposed model formulates the optimal bidding strategy of ESSs considering the real-time energy, flexible ramp-up and ramp-down marginal price signals and the associated uncertainties. In addition, as the market participants cannot directly submit bids for the FRP, the corresponding energy bidding adjustments required to award the proper FRP amounts are elaborated. The mathematical model is linearised and its application in real-time market is investigated. The proposed framework is numerically analysed through which its effectiveness on enhancing the ESS profitability in the real-time electricity markets is verified.

Nomenclature

Indices

s	set of scenarios
t	set of market time-intervals
m	set indicating the slope of each block in the piece-wise linearised flow-power function of ESS
rt	real-time market
fru	flexible ramping up
frd	flexible ramping down
de,ch	discharging and charging modes
u,d	superscripts denoting increase and decrease

Parameters

λ^e	forecasted energy price
$\lambda^{\text{fru}}, \lambda^{\text{frd}}$	forecasted FRU and FRD prices
Ω_s	probability of scenario s
pr^f	probability of ESS failure
δ^e	penalty of not providing the awarded power output
$\delta^{\text{fru}}, \delta^{\text{frd}}$	penalty of not providing FRU and FRD
C^{ch}	start up cost of ESS in charging mode
P	power level traded in DAM
$\underline{P}, \overline{P}$	minimum and maximum power levels
$\underline{q}, \overline{q}$	minimum and maximum water flow levels
$\overline{q}^m$	maximum water flow of block m in the piece-wise linearised flow-power function of ESS
$\underline{\text{SOC}}, \overline{\text{SOC}}$	minimum and maximum state of charge of ESS
SOC_T^{da}	state of charge at T based on the energy trade in DAM
l^m	slope of block m in the piece-wise linearised flow-power function
ξ	round-trip efficiency of the ESS
α	confidence level for which the profit is higher than ϕ
β	factor of risk aversion
$I^{\text{de}}, I^{\text{ch}}$	binaries indicating the state of operation of ESS in DAM (1: yes, 0:no)

Decision variables

Δp^{rt}	change of power output in RTM
p	power output of the ESS
ru,rd	desired flexible ramping up and flexible ramping down levels
$ru^{\text{de}}, rd^{\text{de}}$	provided flexible ramping up and down in discharging mode
$ru^{\text{ch}}, rd^{\text{ch}}$	flexible ramping up and down in charging mode
cu^{ch}	start up cost incurred in RTM in charging mode
q	water flow of the ESS
q^m	water flow of block m in the piece-wise linearised flow-power function of ESS
soc	state of charge of the ESS
Π_s	expected profit of scenario s
ϕ	auxiliary variable for CVaR
ψ_s	auxiliary variable indicating the excess of profit over ϕ in scenario s
$CVaR$	critical value at risk
$y^{\text{de}}, y^{\text{ch}}$	binaries indicating the state of operation of ESS in RTM (1: yes, 0:no)
$x^{\text{de},u}, x^{\text{de},d}$	binaries indicating increase and decrease in discharging power output in RTM (1: yes, 0:no)
$x^{\text{ch},u}, x^{\text{ch},d}$	binaries indicating increase and decrease in charging power output in RTM (1: yes, 0:no)

1 Introduction

Intermittency and variability in renewable generations may impose serious challenges in modern power systems, precise solutions to which should be sought or it may otherwise lead to immense supply curtailments, load outages and market price spikes [1, 2]. This calls for new strategies and practical mechanisms for secured operation of the power grids with massive integration of

renewables; in particular, additional flexibility should be planned and introduced to different sectors in the grid, so the system operators can ensure that the supply is continuously able to follow and meet the stochastic demand [3–5]. Research efforts on efficient technologies and mechanisms to improve system flexibility have seen a tremendous growth in recent years. Among different technologies, energy storage systems (ESSs) bring about potentials for significant operational flexibility and have been realised as an effective solution to overcome the intermittency concerns of renewable generations [6, 7]. Among the prominent advantages of such technologies in modern power systems, one can highlight the ESS ability to smoothen the energy market prices, defer transmission line expansion decisions, enhance the system reliability and resilience and so on [8, 9].

The ESSs may be owned either by system operators or private investors. In the former, the ESSs are primarily employed for cost-effective operations and enhanced system-wide reliability [10, 11]. In the latter, however, investors are impressively attracted by the profitability of ESS solutions in electric industry, the increment of which depends on the optimal site and size of the ESS in the system [12, 13]. Dvorkin *et al*. [12] have presented a bi-level optimisation model to determine the optimal site and size of the ESSs in the grid, the solutions to which not only reduce the investment costs, but also lead to an improved system operating costs. In addition to the optimal sizing and siting of ESS solutions, the profitability is also derived by the precise forecasts of market behaviour and bidding strategies. The notable works in this area are [14–20]. A bidding strategy for battery ESSs is suggested in [14] to simultaneously participate in day-ahead energy, spinning reserve and regulation markets. Robust optimisation is applied to model the market prices and the energy procurement in reserve and regulation services. Nojavan *et al.* [15] have assessed the profitability of compressed air energy storage in the day-ahead and real-time energy arbitrage markets. They proposed a stochastic optimisation for the day-ahead market (DAM) and a robust model for the real-time market (RTM). In [16], the authors have proposed a demand response participation framework for wind power combined with energy storage aiming at leveraging the joint profitability. The optimal joint participation of solar power plant and energy storage in energy and reserve markets is developed in [17]. On this basis, the authors developed a model predictive control approach considering the potential uncertainties, e.g. solar power output and market prices.

Recently, a new market product named flexible ramping product (FRP) is introduced in a number of modern electricity markets, California ISO (CAISO) in particular, which aims to enhancing the market flexibility. The FRP is essentially the energy capacity of RTM players which is reserved to handle the stochastic net-load (i.e. the demand minus intermittent supply) uncertainties and variability in the next immediate time-interval [21–23]. Since ESSs are considered among the fast-response flexible resources, this product can bring about a significant opportunity to gain higher economic gains and financial benefits, only if its unique features are well understood and precise bidding strategies are effectively established. Conversely, if the ESS owners as well as the other market players do not make informed decisions to participate in the FRP market, they may encounter financial losses. In contrast with other market products (e.g. energy and ancillary services), the bidding strategies in the FRP market would be more complicated as the players may not submit economical bids. In fact, the FRP marginal prices are determined according to the marginal energy opportunity costs [23, 24].

In order to benefit from FRP market, Hu *et al.* [25] have suggested a framework in which the ESS participates in the day-ahead energy and FRP markets. Moreover, Wang *et al.* [26] have proposed a bidding strategy for participation of microgrids in joint day-ahead energy, reserve and FRP markets. However, these studies do not consider the fact that FRP is a RTM product and is not procured in the DAM. Also, they do not offer any economic bidding strategy (amount along with the associated price) to award the desired amounts of energy and FRP. Different from the past research, this paper suggests an informed decision framework for ESSs participation in the FRP market. The proposed linearised mathematical model is centred on stochastic real-time price-based unit commitment (PBUC) of the ESSs developed based on the real-time energy, flexible ramp up (FRU), and flexible ramp down (FRD) marginal price signals. This model is initialised with the energy traded by the ESS in DAM and correspondingly determines the optimal energy and FRP that maximise the ESS profits in RTM. Furthermore, this paper suggests an effective bidding strategy for the ESS participation in the RTM. Two case studies with and without FRP mechanisms are investigated, the results of which numerically demonstrate that the ESS profitability is significantly higher in the case with FRP. In summary, the contributions of this paper are presented as follows:

- A risk-averse two-stage stochastic PBUC optimisation formulation for price-taker ESS participation in the RTM is introduced in order to maximise the profitability in the FRP and energy markets. Each scenario consists of different forecasted real-time energy and FRP prices characterised by the corresponding forecast error distribution functions. In order to achieve a tractable optimisation model, a forward probability distance scenario reduction algorithm is used whilst preserving the stochastic characteristics of the original problem. Furthermore, in order to limit the risks of profit loss, the ESS may incur, a well-established risk aversion method named conditional value at risk (CVaR) is implemented.
- As the market participants do not bid for FRP directly, a modified energy bidding strategy to achieve a profitable ESS participation in the RTM is introduced. This step utilises the optimal amounts of energy, FRU and FRD determined by the two-stage optimisation to set the ‘amount’ of each bidding level and employs the associated price forecasts to set the ‘price’ of each bidding level. Provided that the bidding levels are assessed accurately, the ESS can be awarded optimised energy and FRP when the ISO runs the market.
- The IEEE 118-bus test system is implemented to generate real-time energy and FRP price scenarios based on the uncertainties of load and renewable generation. The simulation results infer the impressive efficiency of the suggested approach on the ESS profitability.

The rest of the paper is organised as follows. In Section 2, the concept of FRP, its application in RTM and the great opportunity it provides for flexible units to increase their profits are described. The linearised mathematical formulation of the proposed model is presented in Section 3. The bidding strategy of ESS based on energy and FRP price signals in order to maximise its profitability is described in Section 4. The case study and numerical results are investigated in Section 5 and eventually, the concluding remarks are presented in Section 6.

2 Flexible ramping product in real-time market

2.1 Main procedures in real-time markets (RTM)

The RTM process is mainly implemented through real-time unit commitment (RTUC) and real-time dispatch (RTD) procedures. Both RTUC and RTD are multi-interval optimisation problems, where only the outcome of the first time-interval optimisation is critically requisite for market players and those of other intervals are solely advisory to participants to schedule their resources accordingly. The RTUC comprises of 15 min time-intervals and can determine the unit commitment commands (on/off) for rapid-start generating units, for which the minimum up and down timings are less than the RTUC time horizon. The RTUC can also determine the dispatch decisions for slower generating units. The RTD is, however, a 5 min process in which only the market players' dispatch profiles are issued. The RTUC market time-horizon is set to include all the intervals until the end of the next hour. On this basis, the market horizon alters from 60 to 105 min and the number of intervals alters from 4 to 7 [21].

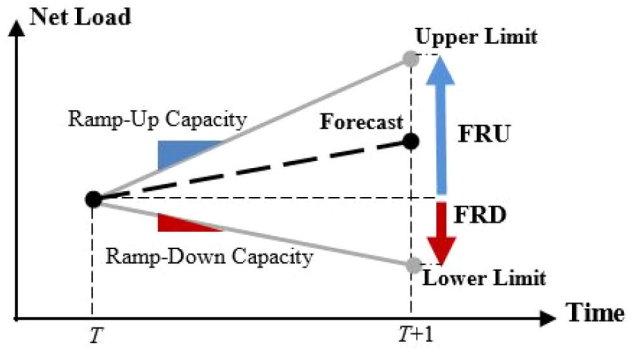

Fig. 1 *FRP procurement according to net-load forecast errors [29]*

2.2 Prime features of the flexible ramping product

The FRP is procured in both RTUC and RTD processes based on the corresponding net-load forecast errors. In each optimisation process, the ISO assures that the supply is able to meet the net-load uncertainties in the next-immediate market time-interval. In particular, the ISO evaluates, at time T, the net-load forecast accuracy at $T+1$ and the available ramping flexibility in response to the forecast error (see Fig. 1). To be able to follow a large range of net-load forecast error at $T+1$, the ISO may reserve additional ramping capacities (FRU for upward and FRD for downward) at time T [27, 28].

The FRP is realised via reserving the energy capacity of the RTM players. In other words, if the system ramping capability is not sufficient, the ISO reserves additional ramping from the energy capacity that players have submitted to the real-time energy market. In this respect, the ISO compensates those players who missed the chance to sell/buy energy in the market, but their energy capacity is reserved for FRP. The opportunity cost corresponding to this participation in energy market is paid to those players providing FRP [29]. The energy opportunity cost is the difference between the market clearing price (MCP) and the player's submitted bid for energy. The highest opportunity cost for FRU procurement is the FRU marginal price, while it is the FRD marginal price for FRD procurement. All units providing FRU or FRD are compensated according to the associated marginal prices [29].

3 Mathematical formulation

3.1 Two-stage stochastic optimisation

Tailored to the pumped hydro storage (PHS) units, we propose a mathematical model for ESS participation in the FRP market. Since the ESSs are relatively small-sized compared to other market participant such as thermal generating units, their energy and ancillary services trades do not affect the energy locational marginal prices. Hence, we consider the ESSs to be price-taker. Note that although the operational constraints of the PHSs are modelled here, the proposed framework is generic enough to accommodate other types of ESSs by modifying the related constraints. We assume that the ESS has participated in DAM and the associated energy schedule is considered as the input to the RTM. The ESS owner is seeking to maximise its profit in RTM according to the forecasts of MCP, FRU and FRD marginal prices. Thus, the objective function (C) in the proposed optimisation model is

$$\begin{aligned} C = \mathbb{E}(\Pi_s) = \max \Big[& (\Delta t(\Delta p_1^{rt}\lambda_1^e + ru_1\lambda_1^{\text{fru}} + rd_1\lambda_1^{\text{frd}} \\ & - pr_1^f(p_1\delta_1^e + ru_1\delta_1^{\text{fru}} + rd_1\delta_1^{\text{frd}})) - cu_1^{\text{de}} \\ & + \sum_{s=1}^{S}\Omega_s\sum_{t=2}^{T}\Big(\Delta t(\Delta p_{s,t}^{rt}\lambda_{s,t}^e + ru_{s,t}\lambda_{s,t}^{\text{fru}} + rd_{s,t}\lambda_{s,t}^{\text{frd}} \\ & - pr_t^f(p_{s,t}\delta_t^e + ru_{s,t}\delta_t^{\text{fru}} + rd_{s,t}\delta_t^{\text{frd}})) - cu_{s,t}^{\text{de}}\Big)\Big] \end{aligned} \tag{1}$$

The proposed objective function is a two-stage problem, the first stage of which determines the optimal energy, FRU and FRD levels that may be awarded by participating in the first interval of RTM. The second stage evaluates the estimated profit the ESS can make in the next intervals of the RTM. Also, it is assumed that the ESS has a perfect forecast of the price signals in the first stage. Note that the optimisation time-horizon set by T is assumed to be equal to the RTUC time-horizon which fluctuates between 4 and 7 upon the time (hour) and spans to the end of the next trading hour. The proposed objective function is subject to the following constraints.

The operating status of ESS in generation, consumption and idle modes of operation are modelled in (2)

$$y_{s,t}^{\text{de}} + y_{s,t}^{\text{ch}} \le 1 \qquad \forall s,t \tag{2}$$

The start-up cost constraints in ESS pumping mode are enforced as follows:

$$cu_{s,t}^{\text{ch}} \ge C^{\text{ch}}(y_{s,t}^{\text{ch}} - y_{s,t-1}^{\text{ch}}) \quad \& \quad cu_{s,t}^{\text{ch}} \ge 0 \quad \forall s,t \tag{3}$$

The difference between the ESS output power in the RTM and that in the same time-interval in DAM comes primarily from either generation or consumption power level variations

$$\Delta p_{s,t}^{rt} = \Delta p_{s,t}^{\text{de},u} - \Delta p_{s,t}^{\text{de},d} - \Delta p_{s,t}^{\text{ch},u} + \Delta p_{s,t}^{\text{ch},d} \qquad \forall s,t \tag{4}$$

The variables $\Delta p^{\text{de},u}$ and $\Delta p^{\text{de},d}$ stand for the increase or decrease in power output in discharging mode in RTM. Likewise, $\Delta p^{\text{ch},u}$ and $\Delta p^{\text{ch},d}$ show the same in charging mode. On this basis, the ESS generating and consumption power level constraints in the RTM are represented as follows:

$$p_{s,t}^{\text{de}} = P_t^{\text{de}} + \Delta p_{s,t}^{\text{de},u} - \Delta p_{s,t}^{\text{de},d} \quad \forall s,t \tag{5}$$

$$p_{s,t}^{\text{ch}} = P_t^{\text{ch}} + \Delta p_{s,t}^{\text{ch},u} - \Delta p_{s,t}^{\text{ch},d} \quad \forall s,t \tag{6}$$

Note that parameters P^{de} P^{ch} indicate the traded discharging and charging energies in DAM which is binding in RTM. The change in the ESS output power in its generating state in RTM is limited by the following constraints:

$$(1 - I_t^{\text{de}})x_{s,t}^{\text{de},u}\underline{P}^{\text{de}} \le \Delta p_{s,t}^{\text{de},u} \quad \forall s,t \tag{7}$$

$$\Delta p_{s,t}^{\text{de},u} \le x_{s,t}^{\text{de},u}(\overline{P}^{\text{de}} - P_t^{\text{de}}) \quad \forall s,t \tag{8}$$

$$0 \le \Delta p_{s,t}^{\text{de},d} \le x_{s,t}^{\text{de},d}P_t^{\text{de}} \quad \forall s,t \tag{9}$$

$$x_{s,t}^{\text{de},u} + x_{s,t}^{\text{de},d} \le 1 \quad \forall s,t \tag{10}$$

In which, $x_{s,t}^{g,u}$ and $x_{s,t}^{g,d}$ are the binaries indicating if the ESS decides to increase or decrease its generating power output in the RTM (1: yes, 0: no). According to (7), only if the ESS is not in its generation mode in DAM ($I_t^{\text{de}} = 0$), $\Delta p_{s,t}^{\text{de},u}$ should be greater than the minimum generating power ($\underline{P}^{\text{de}}$). As in (8), the maximum increase in the ESS output power is limited to the difference between maximum accessible power and that traded in DAM at the same time-interval (P_t^{de}). The maximum decrease in ESS generation power is limited, in (9), to P_t^{de}. The auxiliary binaries $x_{s,t}^{\text{de},u}$ and $x_{s,t}^{\text{de},d}$ are enforced in (10) to prevent the ESS generation level to decrease and increase at the same time. In the case of an increment in the ESS generation, $x_{s,t}^{\text{de},u}$ will be equal to 1 and $x_{s,t}^{\text{de},d}$ otherwise. Similar constraints are enforced representing the ESS pumping state

$$(1 - I_t^{\text{ch}})x_{s,t}^{\text{ch},u}\underline{P}^{\text{ch}} \le \Delta p_{s,t}^{\text{ch},u} \quad \forall s,t \tag{11}$$

$$\Delta p_{s,t}^{\text{ch},u} \le x_{s,t}^{\text{ch},u}(\overline{P}^{\text{ch}} - P_t^{\text{ch}}) \quad \forall s,t \tag{12}$$

$$0 \le \Delta p_{s,t}^{\mathrm{ch},d} \le x_{s,t}^{\mathrm{ch},d} P_t^{\mathrm{ch}} \quad \forall s,t \tag{13}$$

$$x_{s,t}^{\mathrm{ch},u} + x_{s,t}^{\mathrm{ch},d} \le 1 \quad \forall s,t \tag{14}$$

The ESSs can provide FRP in both generating and pumping states, the constraints of which are suggested in the following:

$$ru_{s,t} = ru_{s,t}^{\mathrm{de}} + ru_{s,t}^{\mathrm{ch}} \quad \forall s,t \tag{15}$$

$$rd_{s,t} = rd_{s,t}^{\mathrm{de}} + rd_{s,t}^{\mathrm{ch}} \quad \forall s,t \tag{16}$$

$$p_{s,t}^{\mathrm{de}} + ru_{s,t}^{\mathrm{de}} \le \overline{P}^{\mathrm{de}} y_{s,t+1}^{\mathrm{de}} \quad \forall s,t \tag{17}$$

$$p_{s,t}^{\mathrm{de}} - rd_{s,t}^{\mathrm{de}} \ge \underline{P}^{\mathrm{de}} y_{s,t+1}^{\mathrm{de}} \quad \forall s,t \tag{18}$$

$$p_{s,t}^{\mathrm{ch}} + rd_{s,t}^{\mathrm{ch}} \le \overline{P}^{\mathrm{ch}} y_{s,t+1}^{\mathrm{ch}} \quad \forall s,t \tag{19}$$

$$p_{s,t}^{\mathrm{ch}} - ru_{s,t}^{\mathrm{ch}} \ge \underline{P}^{\mathrm{ch}} y_{s,t+1}^{\mathrm{ch}} \quad \forall s,t \tag{20}$$

In (15) and (16), the procured FRU and FRD are evaluated as the summation of the respective amounts in ESS generating and pumping modes. As enforced in (17)–(20), the FRU and FRD are driven by the ESS functional mode at $t+1$, their output power and their lower and upper power limits. Based on (17), the maximum FRU in discharging mode is limited to the difference between the maximum discharging power at t+1 and the output power at t. According to (18), the FRD in discharging mode is limited to discharging power output minus the associated minimum power limit. Likewise, (19) and (20) are enforced for charging mode, except the fact that FRU is procured by a decrease in the output power and FRD is procured by an increase in the output power.

Based on [30], the linearised relationship between the PHS output power and the water flow is presented in the following:

$$\underline{q}^{\mathrm{de}} y_{s,t}^{\mathrm{de}} \le q_{s,t}^{\mathrm{de}} \le \overline{q}^{\mathrm{de}} y_{s,t}^{\mathrm{de}} \quad \forall s,t \tag{21}$$

$$q_{s,t}^{\mathrm{de}} = \underline{q}^{\mathrm{de}} y_{s,t}^{\mathrm{de}} + \sum_{m=1}^{M} q_{s,t}^{\mathrm{de},m} \quad \forall s,t \tag{22}$$

$$0 \le q_{s,t}^{\mathrm{de},m} \le \bar{q}^{\mathrm{de},m} \quad \forall s,t \tag{23}$$

$$p_{s,t}^{\mathrm{de}} = \underline{P}^{\mathrm{de}} y_{s,t}^{\mathrm{de}} + \sqrt{\xi} \sum_{m=1}^{M} q_{s,t}^{\mathrm{de},m} l^{\mathrm{de},m} \quad \forall s,t \tag{24}$$

$$\underline{q}^{\mathrm{ch}} y_{s,t}^{\mathrm{ch}} \le q_{s,t}^{\mathrm{ch}} \le \overline{q}^{\mathrm{ch}} y_{s,t}^{\mathrm{ch}} \quad \forall s,t \tag{25}$$

$$q_{s,t}^{\mathrm{ch}} = \underline{q}^{\mathrm{ch}} y_{s,t}^{\mathrm{ch}} + \sum_{m=1}^{M} q_{s,t}^{\mathrm{ch},m} \quad \forall s,t \tag{26}$$

$$0 \le q_{s,t}^{\mathrm{ch},m} \le \bar{q}^{\mathrm{ch},m} \quad \forall s,t \tag{27}$$

$$p_{s,t}^{\mathrm{ch}} = \underline{P}^{\mathrm{ch}} y_{s,t}^{\mathrm{ch}} + \frac{1}{\sqrt{\xi}} \sum_{m=1}^{M} q_{s,t}^{\mathrm{ch},m} l^{\mathrm{ch},m} \quad \forall s,t \tag{28}$$

Equation (21) ensures the discharging water flow within its limits. In (22), the total water flow in discharging mode is the summation of the water flow amounts of each block m in the linear piece-wise flow-power function which are limited to their maximum values in (23). The linearised relationship of the power and water flow in discharging mode is given in (24). Likewise, the corresponding constraints for the charging mode are set in (25)–(28).

The limits on the stored energy and the water flow are enforced in the following equations:

$$\mathrm{soc}_{s,t} - \mathrm{soc}_{s,t-1} = (q_{s,t-1}^{\mathrm{ch}} - q_{s,t-1}^{\mathrm{de}})/\Delta t \quad \forall s,t \tag{29}$$

$$\underline{\mathrm{SOC}} \le \mathrm{soc}_{s,t} \le \overline{\mathrm{SOC}} \quad \forall s,t \tag{30}$$

Water flow rates are divided by Δt in (29) as the real-time RTUC and RTD are run in 15 and 5 min time-intervals, respectively.

In order to ensure that there is always sufficient stored energy and the ESS is able to provide the scheduled energy at DAM, it is assumed that the stored energy at time T in RTM optimisation is greater than equal to its value at the same time-interval in DAM. This is enforced in the optimisation model in the following equation:

$$\mathrm{soc}_{s,T} \ge \mathrm{SOC}_T^{da} \tag{31}$$

3.2 Risk-aversion measure

The risk-aversion measure CVaR is implemented in order to limit the decision-making risks. For a scenario-based stochastic optimisation model, the CVaR can be evaluated by the following optimisation:

$$\mathrm{CVaR} = \min \left(\phi + \frac{1}{1-\alpha} \sum_{s=1}^{S} \Omega_s \psi_s \right) \tag{32}$$

Subject to:

$$\phi - \Pi_s \le \psi_s \quad \forall s \tag{33}$$

$$\psi s \ge 0 \quad \forall s \tag{34}$$

Here, α sets the confidence level for which the profit will be higher than the value at risk ϕ. In other words, the probability that the objective function is greater than or equal to ϕ is lower than or equal to $(1-\alpha) \times 100\%$. Besides, ψ_s indicates the excess of profit over ϕ in scenario s.

In order to have control over the risk factor of the optimisation, the risk measure (32) subject to (33), (34) can be embedded in (1) using the coefficient β ($0 \le \beta \le 1$) as follows:

$$\begin{aligned} C = \ & \max \ (1-\beta) . \Pi_s - \beta . CVaR = \\ & \max \ (1-\beta) . \Pi_s - \beta . \left(\phi + \frac{1}{1-\alpha} \sum_{s=1}^{S} \Omega_s \psi_s \right) \end{aligned} \tag{35}$$

The objective function (35) along with constraints (2)–(31), (33) and (34) comprise the stochastic optimisation we propose for the participation of ESSs in the real-time energy and FRP market. The optimal values of the decision variables $\{\Delta p_1^{rt}, ru_1, rd_1, y_1^{\mathrm{de}}, y_1^{\mathrm{ch}}\}$ along with the RTM price forecasts $\{\lambda_1^e, \lambda_1^{\mathrm{fru}}, \lambda_1^{\mathrm{frd}}\}$ comprise the inputs needed for the proposed bidding strategy in Section 4.

4 Proposed bidding strategy for FRP

The suggested real-time PBUC optimisation for ESSs participation in RTM, presented in Section 3, only specifies the optimal change in power as well as the FRU and FRD values based on the corresponding forecasted price signals. The ESSs, however, should decide about their bidding strategies for effective and profitable participation in different markets. This participation strategy is highly dependent upon the bids that the ESS owner submits to the market. Market players are, however, not able to submit bids in FRP and the ISO determines the FRU and FRD allocated to the players according to their energy opportunity cost. This makes the ESSs bidding strategy a complicated challenge. On this basis, in this section, a method is proposed to set the price of each level in the energy bid with the aim of optimal energy and FRP procurement using the bidding input obtained from the optimisation proposed in Section 3.

Here is the procedure that the ISO follows to allocate the FRU and FRD to market participants: at each point in time, the ISO specifies the required FRU and FRD according to the net-load

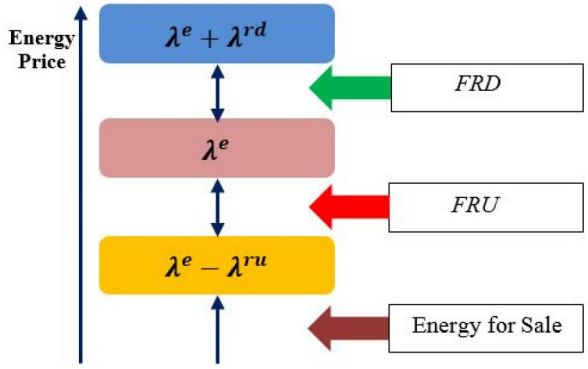

Fig. 2 *Bidding strategy to achieve the optimal FRP and energy in State I (increase in ESS generation or decrease in its consumption level)*

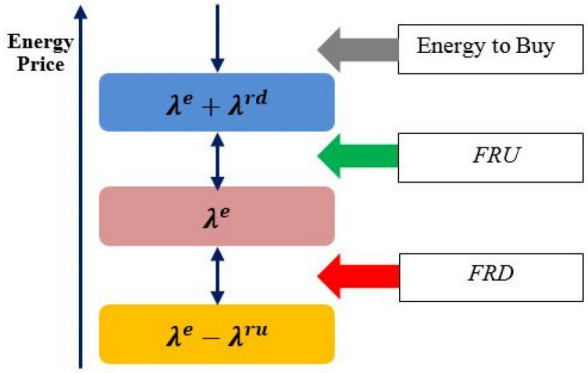

Fig. 3 *Bidding strategy to achieve the optimal FRP and energy in State II (decrease in ESS generation or increase in its consumption level)*

Table 1 Energy storage unit data

$\underline{q}^g$ & $\underline{q}^p$,	$\bar{q}^g$ & $\bar{q}^p$,	c^g,	c^p,
Hm^3/h	Hm^3/h	$	$
7	20	100	200
$\underline{SOC}$,	$\bar{SOC}$,	SOC_0 & SOC_f,	ξ
Hm^3	Hm^3	Hm^3	
60	200	80	0.9

forecast error function and values [29]. The ISO then determines the FRP for market participants based on their submitted energy capacity and relevant prices. In fact, the ISO reserves the energy capacity of market player to procure the required FRP. The following significant considerations are critical to success of this mechanism [21, 29]:

- As the main target, the ISO should run the market to minimise the system operational costs.
- The conventional RTM participants submit hourly bids to the market while the ISO runs a multi-interval market process where the decision of the first interval is binding. For the sake of profitability and flexibility to manage the impacts of uncertainties on the price signals and ESS resources, it is assumed that the ESSs have the option to modify their bids at each RTM step.
- If the system ramping flexibility is not sufficient to respond to the forecasted net-load uncertainties, the ISO will procure additional FRP by reserving the players' energy capacity, which is the power generation or consumption level that the player has specified in its submitted bid to RTM. This continues until the FRU and FRD constraints are satisfied.
- The ISO should pay FRU and FRD procurement costs to the market players according to their energy opportunity costs. The maximum opportunity cost for providing FRU and FRD will be their respective marginal prices.

Providing the FRP with minimum operation costs will help reserving the energy capacity of the market players whose bids are the closest to the MCP. In fact, if the energy capacity of the less-expensive units is reserved for FRP, more expensive units will be called to provide the required energy, resulting in a higher system operation cost. Furthermore, FRP provision by more expensive units will minimise the energy opportunity costs and, accordingly, the FRP marginal prices. The FRP process continues by reserving the energy capacity of the players for which the difference between their bids and MCP is greater. Hence, all the submitted generation bids less than the difference between the MCP and FRP marginal price will be considered for energy generation and the bids greater than MCP plus FRP marginal price will be accounted for energy consumption. Besides, the submitted generation bids between MCP and MCP minus FRP marginal price and those for energy consumption between MCP and MCP plus FRP marginal price will be reserved for the FRP services.

To achieve an optimal energy and FRP values in the market, the ESS should submit an *energy bid* following the real-time PBUC optimisation which should comprise at least two price levels, one for energy and the other for FRP. According to Figs. 2 and 3, the ESS bid is submitted according to its desired change in its output power level (Δp_t^{rt}) which could be divided into two different states:

- State I ($\Delta p_t^{rt} \geq 0$): This state indicates an increase in the generation or a decrease in consuming power. According to Fig. 2, the ESS should submit one bid to sell its energy to the market with a power level equal to Δp_t^{rt} and a price less than $\lambda^e - \lambda^{\text{fru}}$. To ensure an FRU, it should submit a bid to sell its energy with power level equal to the desired FRU and a price between λ^e and $\lambda^e - \lambda^{\text{fru}}$. Such a bid ensures the ESS ability to provide ramp-up services either by increasing its generating power or decreasing its consumption power. Finally to enable an FRD, the ESS should submit a bid to buy energy with power level equal to the desired FRD and a price between λ^e and $\lambda^e + \lambda^{\text{frd}}$. This bid indicates the ESS ability to provide ramp-down capacity by decreasing its generating power or increasing its consumption level.
- State II ($\Delta p_t^{rt} \leq 0$): This state represents a decrease in ESS power generation or an increase in its power consumption level. According to Fig. 3, the bid should be greater than $\lambda^e + \lambda^{\text{frd}}$ with the energy capacity equal to $-\Delta p_t^{rt}$ in order to approach an optimal energy purchase. The FRU will be enabled if the ESS submits a bid with power level equal to the desired FRU value and a price between λ^e and $\lambda^e - \lambda^{\text{fru}}$. Similarly, the ESS should submit another bid with a power level equal to FRD and a price between λ^e and $\lambda^e + \lambda^{\text{frd}}$, if FRD is to be gained.

5 Case studies and numerical results

5.1 Critical assumptions

The proposed real-time PBUC optimisation model is implemented on a PHS, the data of which are provided in Table 1 [31]. The focus is on the ESS profitability from participation in the RTM through its optimal awards of FRP and energy. Note that since the ISOs attempt to procure 100% of their ancillary services in the DAM, particularly spinning and non-spinning reserves as well as regulation reserves [29], it is assumed that the ESS only participates in the RTM in order to award energy and FRP. Hence, the ESS involvement in the real-time reserve and regulation markets is neglected in this study. It is also assumed that the ESS has participated in DAM and its traded energy in DAM time-intervals is considered known as the initial values in the RTM. The values of α and β are assumed 0.95 and 0.5, respectively.

The system under study is the IEEE 118-bus test system whose data are given in [31]. As the FRP is only procured during normal operating conditions (and not during emergencies), the contingency scenarios are not considered. DC power flow model is implemented to run the RTM in which the transmission lines power

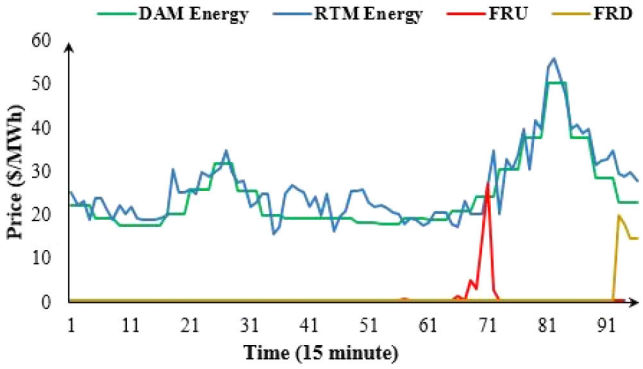

Fig. 4 *Price signals including: DAM and RTM energy prices as well as FRU and FRD marginal prices. The real-time prices are the average of the ten MCS cases*

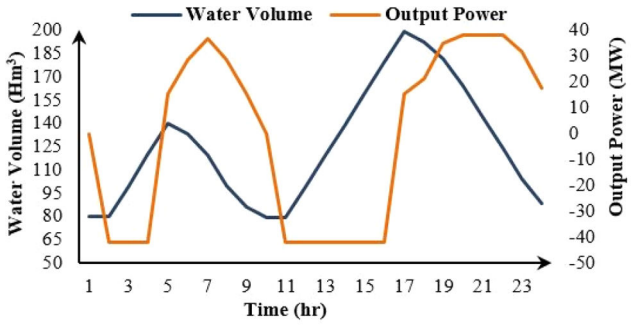

Fig. 5 *ESS stored energy and output power based on the energy traded in DAM*

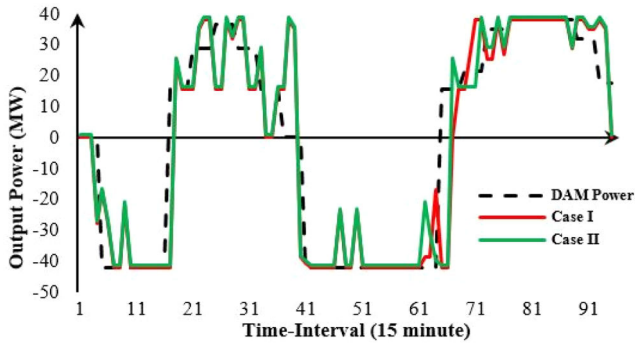

Fig. 6 *Average of ESS output power in RTM in two case studies: Case I (without FRP) and Case II (with FRP)*

capacity limits are taken into account. The generating units submit energy bids in DAM and RTM based on their power-cost functions. The original model was quadratic which was linearised with five steps. The piece-wise linear power-cost function was used as their bid in DAM and RTM. For wind generators, it is assumed that their bidding price is 0, i.e. they sell with any market price. For loads, it is assumed that they purchase the demands up to the price cap of 1000$/MWh.

In order to increase the net-load intermittency and the need for FRP, the wind energy percentage is assumed to be 25% of the load. The confidence level for the net-load forecast error coverage is 95% based on the current CAISO's practice and it is considered that the FRP dispatch (energy under FRU and FRD) is distributed among all the FRP providers proportional to their share of the total procured FRP. The load and wind forecast error probability distributions are assumed to follow normal distribution functions. These normal functions have means equal to the day-ahead forecasted value and the standard deviations provided below [24]:

- Day-ahead: 1% load, 10% wind.
- Real-time: 0.15% load, 1% wind.

In this case study, it is assumed that the ESS has access to the grid model and is able to run a synthetic market to attain such forecasts. With this in mind and in order to generate scenarios, seven steps were assigned to each error probability function. Among the generated scenarios, 30 of them are selected using the forward probability distance algorithm as described in [32]. For each RTM time-interval and for each selected scenario, a deterministic unit commitment optimisation is run for the studied test system whose realised real-time energy, FRU and FRD prices along with the associated probabilities are used as the stochastic parameters to feed in the optimisation model.

In order to reflect the effects of the realised energy and FRP prices on the profitability of the ESS, Monte-Carlo simulation (MCS) is implemented and ten cases are generated. The day-ahead energy price along with the average of real-time energy, FRU and FRD prices resulted from MCS are depicted in Fig. 4.

The simulations were performed in GAMS environment using CPLEX solver on a PC with 7-core processor and 16 GB of RAM and the minimum gap was set to 0.1%. The average computation time is found 349, 423, 537 and 766 s for 4-interval, 5-interval, 6-interval and 7-interval optimisation models, respectively.

5.2 DAM results as input to the RTM scheduling problem

In this section, the output of the ESS participation in DAM is provided. Of important note is that these data serve as the input to the proposed RTM bidding strategy.

The ESS output power and stored energy from its participation in DAM – based on the day-ahead energy prices of Fig. 4 – are illustrated in Fig. 5. It is considered that the PHS stored energy (water behind the dam) at the end of the day amounts equal to its initial value (80 Hm^3). According to Fig. 5, the ESS experienced two transitions to generating state and two transitions to pumping state during the entire day. Besides, the total energy sold by the ESS in DAM is equal to $11317 and the total energy the ESS bought in DAM is equal to $7112. Considering the two transitions to the pumping state with the start-up cost of $200, the ESS total profit from its participation in day-ahead energy market is equal to $3805.

5.3 Real-time simulation results

The following two cases are simulated to assess the ESS profitability when participating in the FRP market:

- Case I: RTM without FRP
- Case II: RTM with FRP

In Case I, the ESS only participates in the real-time energy market, while it jointly participates in both real-time energy and FRP markets in Case II. Note that the energy traded in DAM is employed to initialise the RTM PBUC.

The FRP constraints are modelled earlier in Section 3 which is studied in Case II. In Case I, these FRU and FRD constraints are eliminated from the optimisation model. The average of ESS output power in the ten MCS for this two cases are depicted in Fig. 6. Comparing these values with the real-time energy prices in Fig. 4, it is observed that the RTM change in ESS output power mainly occurs when the real-time energy price fluctuation is highly intense (i.e. time-intervals 20–40, 46–50, 64–75 and 86–96). With these high fluctuations, the ESS's profit in energy market comes primarily from generation in high-price intervals and storage in low-price ones. No new transitions to generating or pumping states occurred in RTM, while all such transitions were observed based on the energy traded in DAM.

The ESS expected profit in each FRP time-interval is presented in Fig. 7. Comparing the results in Figs. 6 and 7, it can be observed that whenever the FRU and FRD marginal prices are 0 (see Figs. 4), the ESS real-time output energy in both cases are the same. On the other hand, when the FRU price is positive, the ESS tends to increase (decrease) its output power in consumption (generating) mode in order to provide additional FRU (see Fig. 6 for the ESS output power in Case I and Case II at time-intervals 64 to 71).

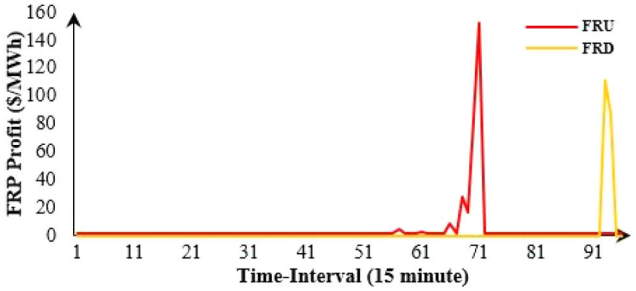

Fig. 7 *FRU and FRD procuremnts and the ESS expected profit in RTM*

Table 2 Two-level bidding strategy to gain FRP and energy

Time	Level 1			Level 2		
	Energy to sell, MW	Energy to buy, MW	Bid price, $/MWh	Energy to sell, MW	Energy to buy, MW	Bid price, $/MWh
66	—	57.6	1000	25	—	17
68	—	—	—	22.54	—	18
69	—	5.9	1000	22.54	—	19
70	—	5.9	1000	22.54	—	13
71	—	5.9	1000	22.54	—	22
93	20.52	—	−100	—	22.54	40
94	17.58	—	−100	—	19.6	−12
95	—	—	—	—	—	—
96	—	—	—	—	—	—

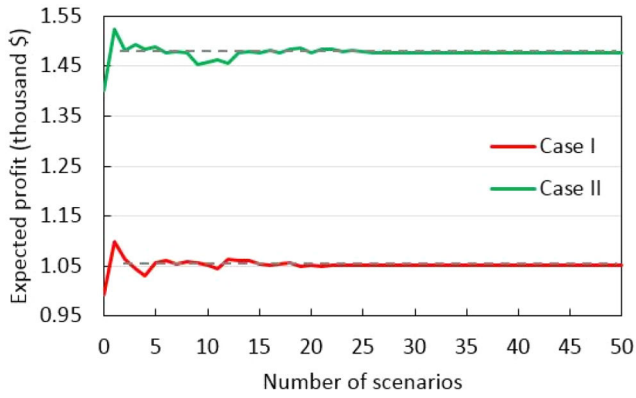

Fig. 8 *Expected profit versus the number of scenarios*

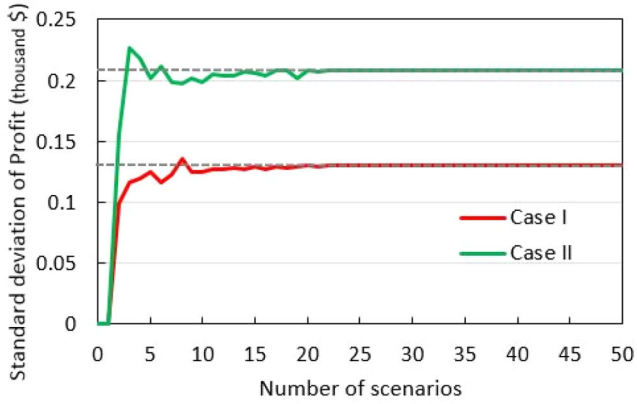

Fig. 9 *Standard deviation of expected profit versus the number of scenarios*

Similarly, whenever the FRD price is positive, the ESS tends to increase its generating power or decrease its pumping power to be able to make a profit by providing FRD. In the studied scenarios, the ESS could not make any profit in time-intervals 95 and 96 as the stored energy in the last time-interval was enforced to be equal to that in the initial state.

The ESS expected profit from participation in real-time energy market is equal to \$1051 and \$999 in Case I and Case II, respectively. It is observed that the ESS profitability in energy market is higher in case without FRP as compared to that with FRP (5.2% higher in this case study). This is due to the change in the ESS output power to provide FRP, which prevented the ESS to practice its optimal participation in energy market. As demonstrated in Fig. 7, the ESS expected profits for providing FRU and FRD are, respectively, \$281 and \$197, amounting a total profit of \$478. Altogether, the ESS expected profit for its participation in RTM are \$1051 and \$1477 in Case I and Case II, respectively. As can be seen, the ESS profitability in RTM through active participation in the FRP market has been significantly increased (40% higher in this case study). Furthermore, considering the DAM participation profit of \$3805, the total ESS profitability will increase from \$4856 to \$5282 (8.8% increment).

5.4 Proposed bidding strategy

To achieve the ESS optimal performance in the market, a bidding strategy for ESS in the RTM is proposed, based on the principles introduced in Section 4. The bidding strategy is implemented on the real-time price signals of Fig. 4 (the average of ten MCS) and is tabulated in Table 2. In this table, the two-level bids (one for energy and one for FRP) when the FRU or FRD prices are greater than 0.5\$/MWh are demonstrated. According to Fig. 4, the FRP prices in time-intervals 66–71 are greater than 0 while the FRD prices are 0. In these time-intervals, the ESS submits a bid to sell its power at a desired FRU (see Table 2: 'Energy to sell' column in Level 2) with a price between the real-time λ^e and $\lambda^e - \lambda^{ru}$, leading to an optimal FRU procurement. Besides, the ESS submits a bid, in the same time-intervals, to buy energy (except in interval 68 where the ESS is in maximum consumption power) with a price lower than $\lambda^e - \lambda^{ru}$, leading to optimal energy values (see Table 2: 'Energy to sell' column in Level 1). Also, the ESS bids at Level 1 helps to free-up its ramp-up or ramp-down capacities, respectively, in its generation or consumption modes, to be able to gain higher FRU profits. As another example in time-intervals 93–96, the FRD price is greater than 0 while the FRU price is 0. In time-intervals 93 and 94, the ESS submits a bid to buy some energy with a price between λ^e and $\lambda^e + \lambda^{rd}$, leading to optimal FRD procurement (see Table 2: 'Energy to buy' column in Level 2). Also, it submits a bid with a price greater than $\lambda^e + \lambda^{rd}$ to achieve the optimal energy values. This bid helps the ESS to free-up its ramp-down capacity and gain a higher FRD profit. In time-intervals 95 and 96, there is no opportunity for ESS profitability in RTM since the stored energy in the last time-interval was enforced to be equal to that in the initial state.

5.5 Analysis on the performance of the proposed method

In this section, two crucial parts of the proposed methodology, namely, selection of number of scenarios and the CVaR performance are analysed and further discussed.

The number of selected scenarios plays a critical role on the precision and effectiveness of the scenario-based optimisation models. This feature is investigated by analysing the expected profit, standard deviation of expected profit and the distance between the reduced set and the original dataset being functions of the number of scenarios. The corresponding results are depicted in Figs. 8–10. As the results suggest, when the number of scenarios exceeds 25, in both Case I and Case II, the expected profit and the associated standard deviation remain stable. In addition, the distance between the reduced scenario set and the original stochastic model after 25 scenarios is reduced to less than 1.2% in Case I and 2.5% in Case II. Note that while our analyses in this particular problem show that selecting equal to or more than 25 scenarios may lead to acceptable results, there exist theoretical works recommending the use of a higher number of scenarios to generate an optimal solution [33, 34]. With the computation time limit requirements (15 min), 30 number of scenarios are here selected.

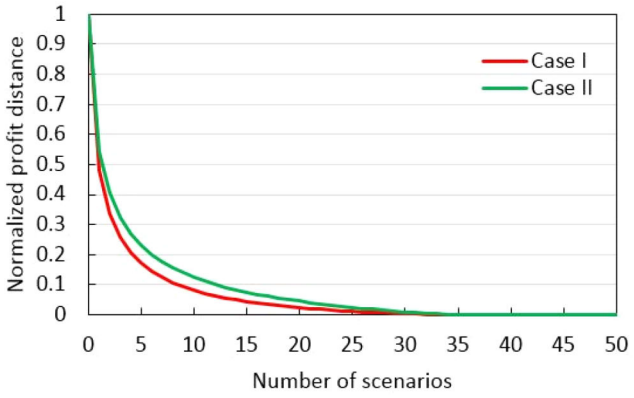

Fig. 10 *Distance between the reduced scenario set and the original dataset as a function of the number of scenarios*

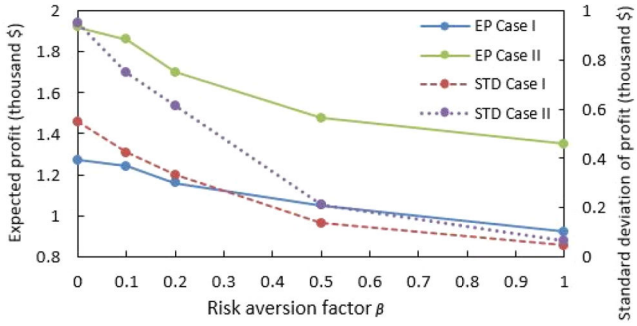

Fig. 11 *CVaR performance as a function of risk aversion factor*

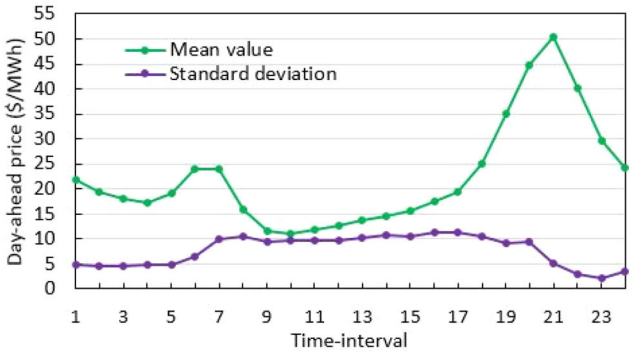

Fig. 12 *DAM historical data of energy prices [35]*

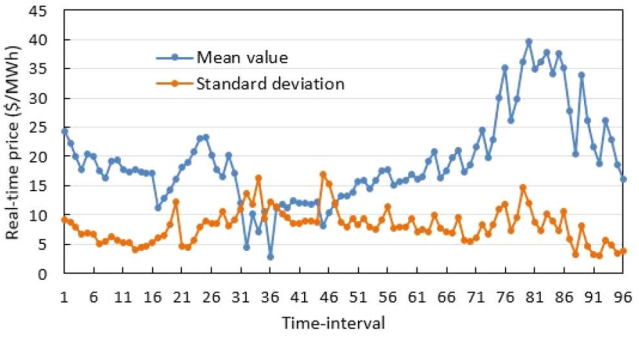

Fig. 13 *RTM historical data of energy prices [35]*

The CVaR risk measure performance is assessed by analysing the expected profit and its associated standard deviation as functions of the risk aversion factor β. The results are depicted in Fig. 11. As can be observed, at the confidence level $\alpha = 0.95$, the point $\beta = 0.5$ approximately can be counted as the knee point of the expected profit curves. At this point, the standard deviation remains in an acceptable range (12.8% of the expected profit in Case I and 14.3% in Case II). Also, after this point, an increase in the risk factor would reduce the expected profit faster than the corresponding standard deviation.

5.6 Real-world case study

The unprecedented proliferation of grid-scale renewables has called for additional ramping procurement (FRU and FRD) in order to effectively and continuously capture the system uncertainties. Higher FRP procurement increases the FRP marginal prices which, in turn, brings about an opportunity for ESS's higher profitability. In this section, a real-world case study whose data are adopted from CAISO, with high-price FRP is presented to assess the out-of-sample performance of the proposed scenario-based framework. The historical DAM and RTM prices, whose mean values and standard deviations are depicted in Figs. 12 and 13, are taken from the market prices in 'Arizona Public Service (AZPS) Balancing Authority Area' of CAISO, node 'OM_LNODEFMR' from 16 May 2018 through 15 June 2018 [35]. Also, the DAM energy prices as well as the real-time energy, FRU and FRD prices for 16 June 2018 (see Fig. 14) used to assess the out-of-sample performance of the proposed framework.

The DAM traded power and the RTM power levels in Case I and Case II are demonstrated in Fig. 15. As can be observed, the ESS output power fluctuation in Case II is lower than that in Case I when the FRP price is non-zero. This highlights the ESS tendency to pursue additional profit by reserving its ramp capacity for FRP (ramp-up for FRU in this case). Comparing the results in Figs. 6 and 15, it is observed that the difference between the ESS real-time output powers in Case I and Case II is much higher in Fig. 15, reflecting the fact that the higher the FRP price is, the lower the profit will be. With this in mind, the ESS expected profits from the energy trading in RTM are \$5129 and \$3211, respectively, in Case I and Case II, revealing a 37% decrement in the RTM energy profitability by the ESS participation in the FRP market. On the other hand, the ESS expected profit for the FRP procurement is \$5053. All in all, the ESS profit due to its participation in RTM in Case II is \$8264 which is 61% higher than that in Case I. Considering the ESS expected profit of \$5437 in DAM, the total expected profit in Case II is 29% higher than that in Case I.

6 Conclusion and discussion

The ESS profitability is a key factor in attracting private investors to finance the energy storage technologies in power grids. The FRP is a recently-introduced service in modern electricity markets, offering a great opportunity for ESSs investors to increase their profits. In this paper, a novel real-time PBUC optimisation model for ESSs participation in FRP markets is proposed via which the ESSs can determine the optimal output power and FRP that must be gained in RTM in order to maximise the profit. The PBUC problem is modelled as a risk-averse two-stage stochastic optimisation, the first stage of which determines the optimal RTM participation strategy and the second stage reflects the effects of uncertainties associated with the energy and FRP prices on the decisions made in the first stage. Furthermore, in order to include the risk impacts on the proposed solutions, the CVaR measure is added to the objective function. Since the FRP will only be procured through ESS energy capacity reserve, this paper also suggests an informed bidding strategy for ESS to submit the optimal energy bids, ensuring that their desired energy and FRP will be realised in RTM. The proposed mechanism is a two-level bidding action that the ESS should submit: one for energy trades and the other for FRP.

The proposed solution is simulated on the IEEE 118-bus test system and MCS is performed to attain the expected real-time realised position. It was observed that the ESS participation in FRP market would result in a 40% increase in the ESS expected profit in RTM. In another case study, the real-word price signals of the CAISO electricity market, in which the FRP prices where relatively high, are used for the ESS scheduling. The simulation results justified the fact that the increase in FRP prices can impressively enhance the ESS profitability in the RTM.

The following subjects are recommended for future research:

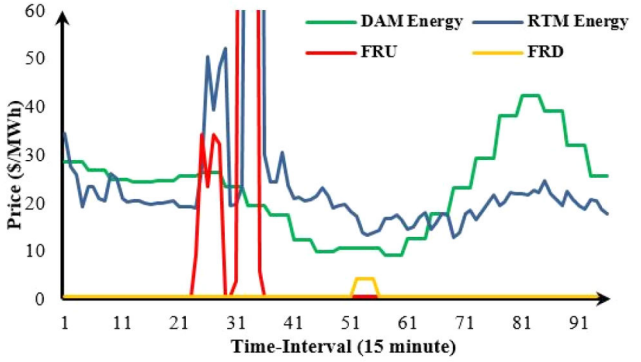

Fig. 14 *Price signals including: DAM and RTM energy prices as well as the FRU and FRD marginal prices. The FRU marginal price in time-intervals 32–34 is 247 $/MWh and the RTM energy prices in time-intervals 33–35 are equal to 169.9, 169.7 and 225.8 $/MWh, respectively*

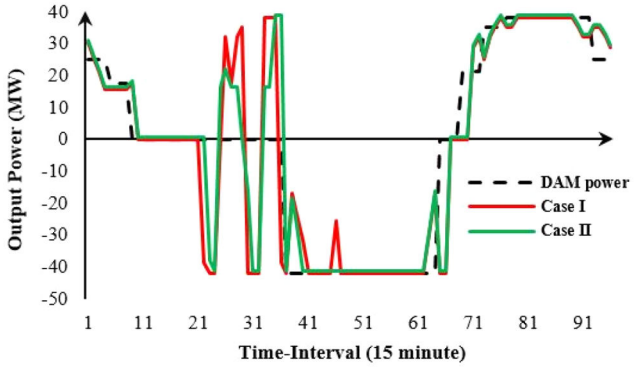

Fig. 15 *ESS output power in RTM in Cases I and II*

• A crucial point in effective ESS participation in joint energy and FRP market is to attain precise forecasts of real-time energy, FRU and FRD prices which was out of the scope of the current work. Future research is recommended to investigate the application of advanced forecast algorithms such as machine learning, specifically tailored to FRP price forecasts and applications in RTM.

• The stochastic problem can be solved as well through chance-constrained and robust optimisation formulations, through which the uncertainties can be addressed effectively. These methods, unlike scenario-based methods, enable dealing with much more scenarios while preserving the computational tractability.

7 Acknowledgment

This work was partially supported by the Iran National Science Foundation (INSF).

8 References

[1] Lu, Z., Li, H., Qiao, Y.: 'Probabilistic flexibility evaluation for power system planning considering its association with renewable power curtailment', *IEEE Trans. Power Syst.*, 2018, **33**, (3), pp. 3285–3295

[2] Helisto, N., Kiviluoma, J., Holttinen, H.: 'Long-term impact of variable generation and demand side flexibility on thermal power generation', *IET Renew. Power Gener.*, 2018, **12**, (6), pp. 718–726

[3] Cochran, J., Miller, M., Zinaman, O., *et al.*: '*Flexibility in 21st century power systems*' (National Renewable Energy Laboratory (NREL), Golden, CO, 2014)

[4] 'Resource flexibility', Available at http://www.energy.ca.gov/renewables/tracking_progress/documents/resource_flexibility.pdf

[5] Papaefthymiou, G., Grave, K., Dragoon, K.: 'Flexibility options in electricity systems'. Project number: POWDE14426, Ecofys, 2014

[6] Nokoobakht, H., Aghaei, J., Shafie-khah, M., *et al.*: 'Assessing increased flexibility of energy storage and demand response to accommodate a high penetration of renewable energy sources', *IEEE Trans. Sustain. Energy*, 2019, **10**, (2), pp. 659–669

[7] Hartwig, K., Kockar, I.: 'Impact of strategic behavior and ownership of energy storage on provision of flexibility', *IEEE Trans. Sustain. Energy*, 2016, **7**, (2), pp. 744–754

[8] Virasjoki, V., Rocha, P., Siddiqui, A.S., *et al.*: 'Market impacts of energy storage in a transmission-constrained power system', *IEEE Trans. Power Syst.*, 2016, **31**, (5), pp. 4108–4117

[9] Nguyen, N., Bera, A., Mitra, J.: 'Energy storage to improve reliability of wind integrated systems under frequency security constraint', *IEEE Trans. Ind. Appl.*, 2018, **54**, (5), pp. 4039–4047

[10] Pandzic, H., Wang, Y., Qiu, T., *et al.*: 'Near-optimal method for siting and sizing of distributed storage in a transmission network', *IEEE Trans. Power Syst.*, 2015, **30**, (5), pp. 2288–2300

[11] Parvini, Z., Abbaspour, A., Fotuhi-Firuzabad, M., *et al.*: 'Operational reliability studies of power systems in the presence of energy storage systems', *IEEE Trans. Power Syst.*, 2018, **33**, (4), pp. 3691–3700

[12] Dvorkin, Y., Fernández-Blanco, R., Kirschen, D.S., *et al.*: 'Ensuring profitability of energy storage', *IEEE Trans. Power Syst.*, 2017, **32**, (1), pp. 611–623

[13] Kelly, J.J., Leahy, P.G.: 'Sizing battery energy storage systems: using multi-objective optimisation to overcome the investment scale problem of annual worth', *IEEE Trans. Sustain. Energy*, 2019, Early access

[14] Kazemi, M., Zareipour, H., Amjady, N., *et al.*: 'Operation scheduling of battery storage systems in joint energy and ancillary services markets', *IEEE Trans. Sustain. Energy*, 2017, **8**, (4), pp. 1726–1735

[15] Nojavan, S., Akbari-Dibavar, A., Zare, K.: 'Optimal energy management of compressed air energy storage in day-ahead and real-time energy markets', *IET Gener. Transm. Distrib.*, 2019, **13**, (16), pp. 3673–3679

[16] Kalavani, F., Mohammadi-Ivatloo, B., Zare, K.: 'Optimal stochastic scheduling of cryogenic energy storage with wind power in the presence of a demand response program', *Renew. Energy*, 2019, **130**, pp. 268–280

[17] González-Garrido, A., Saez-de-Ibarra, A., Gaztañaga, H., *et al.*: 'Annual optimized bidding and operation strategy in energy and secondary reserve markets for solar plants with storage systems', *IEEE Trans. Power Syst.*, 2019, **34**, (6), pp. 5115–5124

[18] Xu, B., Wang, Y., Dvorkin, Y., *et al.*: 'Scalable planning for energy storage in energy and reserve markets', *IEEE Trans. Power Syst.*, 2017, **32**, (6), pp. 4515–4527

[19] Wang, Y., Dvorkin, Y., Fernández-Blanco, R, *et al.*: 'Look-ahead bidding strategy for energy storage', *IEEE Trans. Sustain. Energy*, 2017, **8**, (3), pp. 1106–1117

[20] Kazemi, M., Zareipour, H., Amjady, N.: 'Operation scheduling of battery storage systems in joint energy and ancillary services markets', *IEEE Trans. Sustain. Energy*, 2017, **8**, (4), pp. 1726–1735

[21] 'Business practice manual for market operations. California independent system operator', Oct. 2017. Available at https://bpmcm.caiso.com/BPMDocumentLibrary/Market Operations/BPM_for_MarketOperations_V54_redline.pdf

[22] Khoshjahan, M., Dehghanian, P., Moeini-Aghtaie, M., *et al.*: 'Harnessing ramp capability of spinning reserve services for enhanced power grid flexibility', *IEEE Trans. Ind. Appl.*, 2019, **55**, (6), pp. 7103–7112

[23] Navid, N., Rosenwald, G., Harvey, S., *et al.*: 'Ramp capability product cost benefit analysis', Mid-continental Independent System Operator, June 2013

[24] Navid, N., Rosenwald, G.: 'Ramp capability product design for MISO markets', Market Development and Analysis, 2013

[25] Hu, J., Sarker, M.R., Wang, J., *et al.*: 'Provision of flexible ramping product by battery energy storage in day-ahead energy and reserve markets', *IET Gener., Transm. Distrib.*, 2018, **12**, (10), pp. 2256–2264

[26] Wang, J., Zhong, H., Tang, W., *et al.*: 'Optimal bidding strategy for microgrids in joint energy and ancillary service markets considering flexible ramping products', *Appl. Energy*, 2017, **205**, pp. 294–303

[27] Khoshjahan, M., Moeini-Aghtaie, M., Fotuhi-Firuzabad, M.: 'Developing new participation model of thermal generating units in flexible ramping market', *IET Gener. Transm. Distrib.*, 2019, **13**, (11), pp. 2290–2298

[28] Chen, R., Wang, J., Botterud, A., *et al.*: 'Wind power providing flexible ramp product', *IEEE Trans. Power Syst.*, 2016, **32**, (3), pp. 2049–2061

[29] California Independent System Operator: 'Revised draft final proposal – Flexible ramping product', 2015. Available at http://www.caiso.com/Documents/RevisedDraftFinalProposal-FlexibleRampingProduct-2015.pdf

[30] Li, T., Shahidehpour, M.: 'Price-based unit commitment: a case of Lagrangian relaxation versus mixed integer programming', *IEEE Trans. Power Syst.*, 2005, **20**, (4), pp. 2015–2025

[31] Available at http://motor.ece.iit.edu/Data/PBUCData.pdf

[32] Morales, J., Pineda, S., Conejo, A.J., *et al.*: 'Scenario reduction for futures market trading in electricity markets', *IEEE Trans. Power Syst.*, 2009, **24**, (2), pp. 878–888

[33] Campi, M.C., Garatti, S.: 'The exact feasibility of randomized solutions of uncertain convex programs', *SIAM J. Optim.*, 2008, **19**, (3), pp. 1211–1230

[34] Margellos, K., Goulart, P., Lygeros, J.: 'On the road between robust optimization and the scenario approach for chance-constrained optimization problems', *IEEE Trans. Autom. Control*, 2014, **59**, (8), pp. 2258–22630

[35] Available at http://oasis.caiso.com